International Conference on Applied Energy 2020
Dec. 1 - Dec. 10, 2020, Bangkok / Virtual
Paper ID: 277

Numerical Simulation of Radiation Heat Transfer Characteristics of Oxy-fuel Combustion Furnace

Yan Xie[1,2], Heyang Wang [1,2*], Xin Liu[3], Chaoqun Zhang[3], Jun Zhao[1,2], Junjie Li[1,2]

(1. School of Mechanical Engineering, Tianjin University, Tianjin 300072, China;
2. Key Laboratory of Efficient Utilization of Low and Medium Grade Energy (Tianjin University), Ministry of Education, Tianjin 300350, China;
3. Yantai Longyuan Power Technology Co. Ltd., Yantai 264006, China)

ABSTRACT

In this study, a computational fluid dynamics (CFD) model was developed to study the flow and heat transfer characteristics of a 320 MW oxy-fired boiler with dry and wet flue gas recirculation (FGR). The results show that there exist significant differences in the composition and physical properties of flue gas between the air- and oxy-combustion modes and these differences may lead to remarkable differences in the flow, temperature and heat transfer distributions of boiler. Specifically, since the specific heat of CO_2 and H_2O are higher than that of N_2, the flue gas heat capacity of the oxy-combustion case with wet FGR is significantly higher than the air-combustion case leading to lower furnace temperature and heat absorption of furnace wall. Moreover, since the density of CO_2 is higher than N_2, the overall flow velocity in oxy-fired boiler is lower than that of air-fired boiler, which subsequently affects the boiler flow and temperature distributions in the furnace. The differences in the flow and heat transfer distributions between oxy-fired and air-fired boilers should be taken into consideration when designing new oxy-fuel combustion systems or retrofitting existing air combustion systems to minimize costly modifications to the boiler's heating surfaces.

Keywords: oxy-fuel combustion; radiation heat transfer; flue gas recirculation; coal combustion; numerical simulation

1. INTRODUCTION

Oxy-fuel combustion is recognized as one of the most promising technologies of CO_2 capture [1, 2]. It has been widely studied in small scale problems [3-6]. However, to date the experience on the design and operation of full scale oxy-fired boilers are still rather limited. Experiments on large scale boilers are extremely costly and technically impractical. Then CFD becomes a viable option to study the large scale oxy-fired boilers. In this study we conducted a numerical study on the combustion and heat transfer characteristics of a full scale 320 MW oxy-fired boiler. In oxy-fuel combustion, N_2 is removed by air separation unit (ASU) and coal is burning with the high-purity O_2. The flue gas is then mainly composed of CO_2 and H_2O rather than N_2 in air combustion. Moreover, in order to control combustion temperature, FGR is usually applied to oxy-fuel combustion systems. Depending on if the water vapor is removed from the recirculated flue gas, H_2O concentration in flue gas may also vary over a broad range. Because there exist remarkable differences in the gas properties among N_2, CO_2 and H_2O, the properties of the flue gas mixture (density, heat capacity and radiation properties) of oxy-fuel combustion may significantly differ from those of air combustion. This may dramatically affect the flow, temperature and heat transfer characteristics of oxy-fired boilers. Particularly, in coal-fired boiler radiation is the dominant heat transfer mechanism in the furnace contributing more than 90% of total heat transfer to the furnace water wall [7]. Because of the significantly higher concentration of the absorbing gases, CO_2 and H_2O, the radiation properties of the gas mixture change dramatically. This may strongly affect the furnace heat transfer distribution of the oxy-fired boilers.

Thus, in this study a full scale 320 MW oxy-fired boiler with FGR is numerically studied with particular attention focused on the different furnace wall heat transfer characteristics resulted from different flue gas composition between the air- and oxy-combustion modes. The results from the present study are going to provide guidance to the design of new oxy-combustion systems or retrofit of existing air combustion systems.

Selection and peer-review under responsibility of the scientific committee of the 12th Int. Conf. on Applied Energy (ICAE2020).
Copyright © 2020 ICAE

EnergyXiv-preprint

2. MATHEMATICAL MODELS

ANSYS Fluent is used as the computational platform to implement the CFD models presented in this study. Realizable *k-ε* model is used for turbulence closure [8]. Coal particles are tracked in Lagrangian framework using stochastic tracking method [9]. Coal devolatilization is modeled using a first-order single reaction rate model [10] with the rate parameters obtained from a separate FLASHCHAIN model [11]. The volatile matter is represented by a single virtual substance $C_aH_bO_cS_dN_e$ [12-14]. Assuming that char is composed of pure carbon and ash, the values of *a*, *b*, *c*, *d* and *e* can be determined by the mass balance of each volatile element.

The heterogeneous reactions of char include:

$$C_{char} + 0.5O_2 \rightarrow CO \quad (1)$$

$$C_{char} + CO_2 \rightarrow 2CO \quad (2)$$

$$C_{char} + H_2O \rightarrow H_2 + CO \quad (3)$$

where C_{char} is the carbon in the char. The char surface reaction rate is calculated by the kinetic/diffusion-limited rate model [15] with the rate parameters given in the table below.

Table 1. Char surface reaction rate constants

	Diffusion rate constant	Pre-exponential factor	Activation energy (kJ/mol)
$C + O_2$	4.374×10^{-12}	0.00100	79
$C + CO_2$	2.811×10^{-12}	0.00192	147
$C + H_2O$	2.811×10^{-12}	0.00635	162

The CO and H_2 generated at the char surface are transported to the bulk gas and further oxidized to CO_2 and H_2O. The combustion reaction of the volatile matter $C_aH_bO_cS_dN_e$ is modeled with a two-step reaction scheme. Then the homogeneous reactions include

$$C_aH_bO_cS_dN_e+\left(\frac{a}{2}+\frac{b}{4}-\frac{c}{2}+d\right)O_2\rightarrow aCO+\frac{b}{2}H_2O+dSO_2+\frac{e}{2}N_2 \quad (4)$$

$$CO + 0.5O_2 \rightarrow CO_2 \quad (5)$$

$$H_2 + 0.5O_2 \rightarrow H_2O \quad (6)$$

For most of engineering applications, combustion is extremely intense such that the reaction rate is overall limited by the mixing between the fuel and oxidizer. Thus, Eddy-Dissipation Model (EDM) is used to calculate the homogeneous chemical reaction rates [16, 17].

The Discrete Ordinate Method (DOM) is used to simulate the radiation heat transfer. The emissivity of the gas mixture is calculated using weighted-sum-of-gray-gas model (WSGGM). In WSGGM the emissivity of gas mixture is approximated by the weighted sum of emissivities of several fictitious gray gases,

$$\varepsilon = \sum_{i=0}^{I} a_{\varepsilon,i}(T)\left(1-e^{-k_iPL}\right) \quad (7)$$

where *I* is the total number of fictitious gray gases, $1-e^{-k_iPL}$ is the emissivity of the i^{th} fictitious gray gas over distance *L*, k_i is the absorption coefficient, *P* is the sum of the partial pressures of absorbing gases (CO_2 and H_2O), and $a_{\varepsilon,i}(T)$ is the weighting factor which is approximated as the polynomial of temperature:

$$a_{\varepsilon,i}(T) = \sum_{j=1}^{J} b_{\varepsilon,i,j}\, T^{j-1}\ (i \neq 0) \quad (8a)$$

$$a_{\varepsilon,0} = 1-\sum_{i=1}^{I} a_{\varepsilon,i} \quad (8b)$$

where $J-1$ is the order of temperature polynomial and $b_{\varepsilon,i,j}$ is the polynomial coefficient.

Currently the most widely used WSGGM in combustion CFD was proposed by Smith et al [18] in which the gas mixture is represented by three gray gases ($I=3$) and a third-order temperature polynomial ($J=3$) is used to calculate the weighting factors with the absorption and polynomial coefficients, k_i and $b_{\varepsilon,i,j}$, given as constants respectively for P_w/P_c = 1, 2 and P_c = 0.1 atm, where P_w and P_c are the partial pressures of H_2O and CO_2, respectively. However, in oxy-fuel combustion, CO_2 and H_2O are the major composition of flue gas such that P_c is generally much higher than 0.1 atm. In addition, depending on whether water vapor is removed from the recirculated flue gas, FGR can be operated with dry or wet modes. Different FGR mode will lead P_w/P_c to vary over a broader range. For example, when dry FGR is used, P_w/P_c ~ 0.125, which is far beyond the range of P_w/P_c applicable to the Smith's WSGGM. Since the radiation properties of gas mixture play a critical role in radiative heat transfer calculation, the CFD model needs to adopt an improved WSGGM to account for the effects of gas composition on the emissivity of gas mixture.

In the present study Johansson's WSGGM was implemented into the CFD model framework via a User Defined Function (UDF). In this WSGGM [19, 20], k_i and $b_{\varepsilon,i,j}$ are not constant parameters, but represented as continuous functions of P_w/P_c:

$$k_i = \mathrm{K1}_i + \mathrm{K2}_i\left(\frac{P_w}{P_c}\right) \quad (9)$$

$$b_{\varepsilon,i,j} = \mathrm{C1}_{i,j} + \mathrm{C2}_{i,j}\left(\frac{P_w}{P_c}\right) + \mathrm{C3}_{i,j}\left(\frac{P_w}{P_c}\right)^2 \quad (10)$$

where $\mathrm{K1}_i$, $\mathrm{K2}_i$, $\mathrm{C1}_{i,j}$, $\mathrm{C2}_{i,j}$, $\mathrm{C3}_{i,j}$ are constant coefficients, given in detail in Johansson et al [19, 20]. This model extends the applicability of WSGGM to a much wider range of H_2O and CO_2 partial pressures, and hence,

Copyright © 2020 ICAE
EnerarXiv-preprint

are particularly suitable for the radiation calculation of oxy-combustion problems.

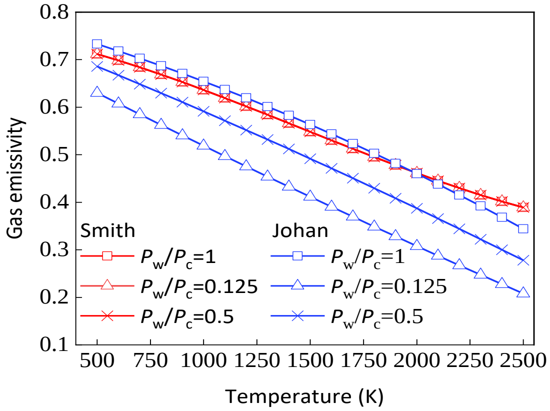

Figure 1. Calculated gas emissivities by Smith and Johansson WSGGM models

Figure 1 shows the values of gas emissivity calculated respectively by the Smith's and Johansson's WSGGMs for different values of P_w/P_c. It is seen that there are remarkable differences in the calculated values of emissivity between the two WSGGMs when P_w/P_c is away from the applicable range of Smith's WSGGM (P_w/P_c = 0.125, 0.5). More importantly, Smith's WSGGM gives the same emissivity values for different P_w/P_c indicating that it cannot properly account for the effect of gas composition on radiation. This illustrates that incorporating Johansson's WSGGM is a critical step for the CFD model to be able to accurately predict the radiation heat transfer of oxy-fired boilers.

With the radiation heat transfer properly accounted in the model, the heat transfer of furnace wall is now determined by the wall thermal boundary condition. In the furnace, the heat absorption from the fire side of boiler is conducted through the furnace wall and then absorbed by the water/steam flow in the water tubes. This heat transfer process can be described as:

$$q = h_{ext}(T_w - T_{ext}) \quad (11)$$

where q is the heat flux through the furnace wall, T_w is the wall surface temperature, T_{ext} is the water/steam temperature in the tubes, h_{ext} is the heat transfer coefficient representing the overall thermal resistance of this heat transfer process [21]. In coal-fired boilers, furnace wall is, more or less, coated with slagged ash. Thus, the value of h_{ext} is largely determined by the thermal resistance of the wall slag layer and typically falls with the range of 300 ~ 600 W/(m^2·K) [21, 22]. Equation (11) defines the thermal boundary condition of the furnace wall. In this study, T_{ext} is 639 K given as the saturated temperature at the drum pressure of 19.78 MPa.g and h_{ext} is 400 W/(m^2·K) determined by a calibration calculation with the boiler steam parameters [21].

3. BOILER GEOMETRY AND OPERATING DATA

Figure 2 shows the schematic of the furnace geometry of the 320 MW boiler with burner and heating surfaces arrangement. The height, width and depth of the boiler are 56.2 m, 14.0 m and 14.0 m, respectively. The mesh is constructed with 4.06 million hexahedral structured cells. This boiler is firing bituminous coal. The coal property data is summarized in Table 2.

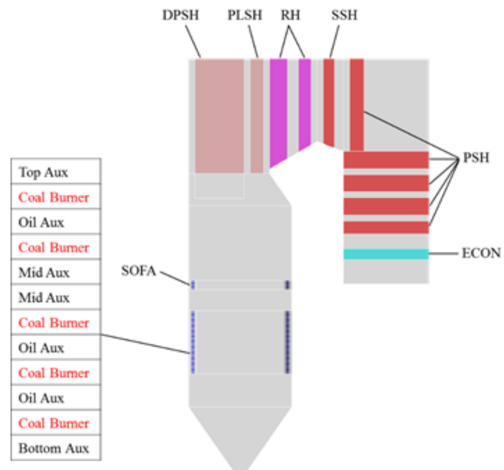

Figure 2. Schematic of the furnace geometry

Table 2. Coal property data (as-received base)

Proximate analysis %		Ultimate analysis %	
Moisture	7.50	C	63.24
Volatile matter	28.63	H	4.08
Fixed Carbon	48.71	O	8.46
Ash	15.16	N	0.75
		S	0.81

Three cases are studied in the present study, including air combustion, oxy-fuel combustion with dry FGR and oxy-fuel combustion with wet FGR, hereafter referred to as Air, Oxy-Dry and Oxy-Wet cases respectively. The model parameters of the Air case are determined based on the design and operating data of the boiler. All three cases use the same the total coal flow rate (123.5 t/h). Different FGR modes (wet or dry FGR) and FGR flow rates affect the furnace inlet O_2 and gas flow rates, and subsequently affect the flow, temperature and heat transfer distributions in the furnace. For the ease of comparison, this study maintain the same burner inlet O_2 and gas mass flow rates for all three cases based on which the needed excess air ratio and FGR ratio for the Oxy-Dry and Oxy-Wet cases can be determined, as shown in Table 3. Here the FGR ratio denotes ratio of recycled flue gas volume flow rate to that of total gas flow and we have assumed that the air used in the oxy-combustion cases is composed of 95% O_2 and 5% N_2 by volume. Note that because the recirculated

Enerarxiv preprint

Copyright © 2020 ICAE

flue gas contains excess oxygen, the excess air ratios of oxy-fuel combustion cases can be significantly lower than that of air-combustion case to maintain the same inlet O_2 flow rate.

Table 3. Excess air ratio, FGR ratio and furnace inlet gas composition

Cases	Air	Oxy-Dry	Oxy-Wet
Excess air ratio	1.235	1.056	1.063
FGR ratio	—	74.30%	77.48%
Inlet gas composition (mole fraction) %			
O_2	20.73	28.57	24.86
H_2O	0.64	--	22.31
N_2	78.63	5.78	4.46
CO_2	--	65.34	48.14
SO_2	--	0.31	0.23

4. RESULT AND DISSCUSION

Figure 3 shows the velocity distributions at the burner inlets and cross-corner section of furnace for different cases. It is seen that the burner inlet velocity of the air-combustion case is higher than those of the oxy-combustion cases which consequently leads to different flow distributions in the furnace. The differences are particularly pronounced between the Air and Oxy-Dry cases. Table 4 gives the volume flow rates and average nozzle air velocities. It shows that the difference in the inlet velocity distributions among the three cases is attributed to the different gas volume flow rates although all cases have the same gas mass flow rates. Since the inlet gas of the oxy-combustion cases contain much higher concentration of CO_2 (as shown in Table 3) and the density of CO_2 is much higher than that of N_2, the inlet gas volume flow rates are lower. Different volume flow rates result in different flow distributions, and will consequently affect the temperature and heat transfer distributions in the furnace.

Table 4. Volume flow rates and average nozzle air velocities under different combustion modes

Case	Volume flow rate m^3/s	Average velocity m/s
Air	68.20	61.68
Oxy-Dry	46.98	42.05
Oxy-Wet	56.41	50.20

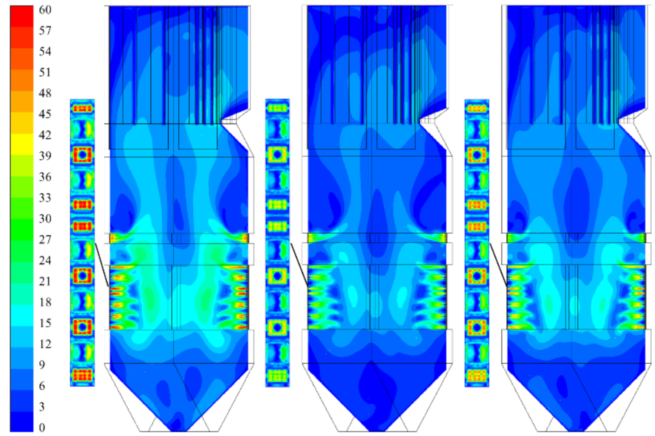

Figure 3. Furnace velocity distributions at the inlets and cross-corner section of furnace

Figure 4 shows the furnace cross-corner sectional temperature distributions for different cases. It is seen that the furnace temperature of the Oxy-Wet case is lower than that of the Air case, while the Oxy-Dry case is slightly higher. The difference in furnace temperature among the three cases is firstly caused by the difference in the specific heat (c_p) of the gas mixture. Table 5 gives the mass fraction of major flue gas composition, specific heat of flue gas (at 2000 K), and total heat absorption of furnace wall of different cases. Note that the c_p of N_2, CO_2 and H_2O (at 2000 K) are 1285 J/(kg·K), 1373 J/(kg·K) and 2839 J/(kg·K), respectively, and that the H_2O concentration of Oxy-Wet case is much higher than the other two cases. Thus the c_p of the gas mixture of Oxy-Wet case is considerably higher than the other two cases, resulting in lower furnace temperature. Since the c_p of CO_2 is only slightly higher than N_2, the large difference in CO_2 concentration between the Oxy-Dry and Air cases only results in slightly higher c_p of the Oxy-Dry case. However, the furnace temperature of the Oxy-Dry case shown in Fig. 4 appears slightly higher than the Air case, opposite to what is expected from the comparison of c_p between the two cases. This can be explained by the differences in flow and furnace temperature distributions between the two cases. As seen in Fig. 3, because the inlet gas velocity of Oxy-Dry case is significantly lower than the Air case, its rotational flow in the furnace is relatively weaker so that the high temperature flame locates near the center of furnace and away from the furnace wall. As seen in Eq. (7), the overall emissivity of flue gas drops exponentially with the path length L. As a result, the overall radiation heat absorption by the furnace wall is reduced (as seen in Table 5) and this effect dominates over that of higher c_p.

EnerarXiv-preprint

 Copyright © 2020 ICAE

As a result, the temperature of Oxy-Dry case appears slightly higher than that of Air case.

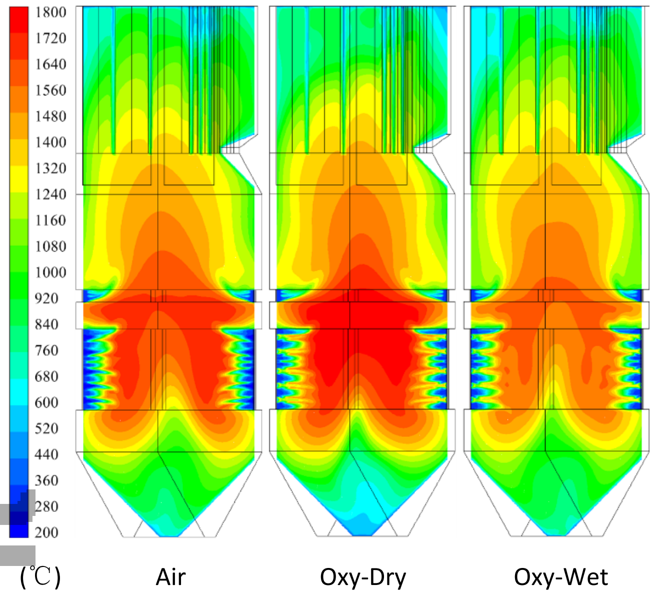

Figure 4. Furnace cross-corner sectional temperature distributions

Table 5. Mass fraction of major flue gas components, specific heat of flue gas, and heat absorption of furnace wall under different combustion modes

	Air	Oxy-Dry	Oxy-Wet
N_2	0.708	0.038	0.034
CO_2	0.207	0.876	0.773
H_2O	0.043	0.039	0.147
c_p (J/kg·K)	1373	1430	1595
Heat absorption (MW)	314.5	297.6	276.2

Figure 5 shows furnace wall heat flux distributions for different cases. Comparing the three cases, it is seen that the peak heat flux of Oxy-Dry case is higher than that of Air case while the Oxy-Wet case is significantly lower, which is consistent with temperature distributions shown in Fig. 4. This is because radiation is proportional to the fourth power of temperature, and hence, becomes extremely sensitive to temperature variations at higher temperatures. As such, the level of peak heat flux is largely determined by the peak flame temperature in the furnace. The heat flux distribution pattern over the entire furnace wall, however, is dependent on the overall furnace temperature distribution. Because the flame of the Oxy-Dry case locates near the center of the furnace, the heat flux in majority of furnace wall area is lower than that of the Air case except for the area corresponding to the location of the highest flame temperature. As a result, the high heat flux region of the Oxy-Dry case is distributed over a smaller area of furnace wall although its peak heat flux is higher. This is the reason why the overall furnace wall heat absorption of the Oxy-Dry case (297.6 MW) is lower than that of the Air case (314.5 MW).

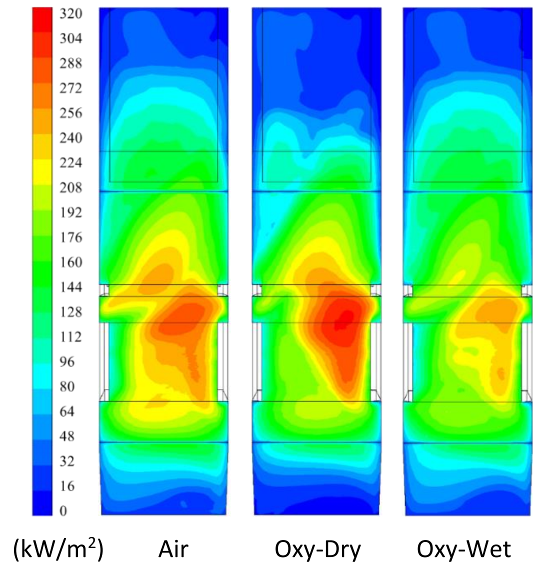

Figure 5. Furnace wall heat flux distributions (front wall)

5. CONCLUSION

A numerical study was conducted on the flow and heat transfer characteristics of a full scale 320 MW oxy-fired boiler. In order to properly account for the impact of different gas composition of oxy-combustion on radiation heat transfer, Johansson's WSGGM was firstly implemented into the CFD model framework to make the CFD model suitable for the radiation calculation of oxy-combustion. Then, numerical studies were conducted for the oxy-fired boiler with both dry and wet FGR. The following conclusions were drawn based on the simulation results:

1. The differences in the composition and physical properties of flue gas between different combustion modes may result in considerable differences in the flow, temperature and heat transfer distributions of boiler.

2. The specific heat of flue gas of oxy-combustion with wet FGR is significantly higher than that of the air-combustion case, leading to lower furnace temperature and reduced furnace wall heat absorption.

3. Because the density of CO_2 is higher than that of N_2, the gas volume flow rate of oxy-combustion with dry FGR is significantly lower than that of air-combustion case which consequently leads to remarkable differences in the furnace flow and temperature distributions.

EnerarXiv-preprint

Copyright © 2020 ICAE

4. The differences in the flow, temperature and heat transfer distributions resulted from the differences in the composition and properties of flue gas of oxy-combustion need to be systematically considered when designing new oxy-combustion or retrofitting existing air-combustion systems.

REFERENCE

[1] Yin C, Yan J. Oxy-fuel combustion of pulverized fuels: Combustion fundamentals and modeling[J]. Applied Energy, 2016, 162: 742-762.

[2] Nakod P, Krishnamoorthy G, Sami M, et al. A comparative evaluation of gray and non-gray radiation modeling strategies in oxy-coal combustion simulations[J]. Applied Thermal Engineering, 2013, 54(2): 422-432.

[3] Guo J, Hu F, Jiang X, et al. Effect of flue gas recycle ratio on radiative heat transfer in a 0.5 MW oxy-fuel combustion furnace[J]. Journal of Engineering Thermophysics, 2019, 40(01): 223-228.

[4] Fujimori T, Yamada T. Realization of oxyfuel combustion for near zero emission power generation[J]. Proceedings of the Combustion Institute, 2013, 34(2): 2111-2130.

[5] Yin C. Refined weighted sum of gray gases model for air-fuel combustion and its impacts [J]. Energy & Fuels, 2013, 27(10): 6287-6294.

[6] Donini A, Bastiaans R J M, Van Oijen J A, et al. A 5-D implementation of FGM for the large eddy simulation of a stratified swirled flame with heat loss in a gas turbine combustor[J]. Flow, Turbulence and Combustion, 2017, 98(3): 887–922.

[7] Steam/its generation and use[M]. 41 ed. Barberton, Ohio, U.S.A: The Babcock & Wilcox Company, 2005.

[8] Schuhbauer C, Angerer M, Spliethoff H, et al. Coupled simulation of a tangentially hard coal fired 700 °C boiler[J]. Fuel, 2014, 122: 149-163.

[9] Boyd R K, Kent J H. Three-dimensional furnace computer modelling[J]. Symposium (International) on Combustion, 1988, 21(1): 265-274.

[10] Badzioch S, Hawksley P G W. Kinetics of thermal decomposition of pulverized coal particles[J]. Industrial & Engineering Chemistry Process Design and Development, 1970, 9(4): 521-530.

[11] Niksa S. Predicting the devolatilization behavior of any coal from its ultimate analysis[J]. Combustion and Flame, 1995, 100(3): 384-394.

[12] Hu Y, Li H, Yan J. Numerical investigation of heat transfer characteristics in utility boilers of oxy-coal combustion[J]. Applied Energy, 2014, 130: 543-551.

[13] Yin C. On gas and particle radiation in pulverized fuel combustion furnaces[J]. Applied Energy, 2015, 157: 554-561.

[14] Wu X, Fan W, Liu Y, et al. Numerical simulation research on the unique thermal deviation in a 1000 MW tower type boiler[J]. Energy, 2019, 173: 1006-1020.

[15] Baum M M, Street P J. Predicting the combustion behaviour of coal particles[J]. Combustion Science and Technology, 1971, 3(5): 231-243.

[16] Magnussen B F, Hjertager B H. On mathematical modeling of turbulent combustion with special emphasis on soot formation and combustion[J]. Symposium on Combustion, 1977, 16(1): 719-729.

[17] Tan P, Tian D, Fang Q, et al. Effects of burner tilt angle on the combustion and NO_X emission characteristics of a 700MWe deep-air-staged tangentially pulverized-coal-fired boiler[J]. Fuel, 2017, 196: 314-324.

[18] Smith T F, Shen Z F, Evaluation of coefficients for the weighted sum of gray gases model[J]. Journal of Heat Transfer, 1982, 104: 602-608.

[19] Johansson R, Andersson K, Leckner B, et al. Models for gaseous radiative heat transfer applied to oxy-fuel conditions in boilers[J]. International Journal of Heat & Mass Transfer, 2010, 53(1-3): 220-230.

[20] Johansson R, Leckner B, Andersson K, et al. Account for variations in the H_2O to CO_2 molar ratio when modelling gaseous radiative heat transfer with the weighted-sum-of-grey-gases model[J]. Combustion and Flame, 2011, 158(5): 893-901.

[21] Wang H, Zhang C, Liu X. Heat transfer calculation methods in three-dimensional CFD model for pulverized coal-fired boilers[J]. Applied Thermal Engineering, 2020, 166: 114633.

[22] Wall T F, Bhattacharya S P, Zhang D K, et al. The properties and thermal effects of ash deposits in coal-fired furnaces[J]. Progress in Energy and Combustion Science, 1993, 19(6): 487-504.

Copyright © 2020 ICAE

EnerarXiv-preprint